Status and Prospects on Top Physics at CDF

BY YUJI TAKEUCHI

Institute of Physics, University of Tsukuba,
Ibaraki, 305-8571,Japan

for the CDF collaboration

Abstract

Since the top quark was discovered at Tevatron in 1994, CDF has been conducting various measurements on top quark properties, including mass, production cross sections, decay modes, kinematical properties, and so on, though they are statistically limited in Run I. Run II in which we can expect at least 20 times higher statistics than Run I, has started in March 2001, and have acquired an amount of data in Run II, comparable to one in Run I. We are at the stage of re-establishing the basic measurements on the top quark and entering exciting Run II era, where precise measurements on top physics, connected to stringent tests of the electroweak theory and search for a new physics beyond the Standard Model are expected. The results of top physics in Run I, and the status and prospects in Run II are reviewed.

1 Introduction

The Collider Detector at Fermilab (CDF) is one of experiments with Tevatron, a $p\bar{p}$ collider at Fermilab. The center of mass energy was 1.8 TeV in Run I, which is increased to 1.96 TeV in Run II.

Fig.1 shows the schematic draw of the CDF IIa detector. The CDF IIa detector consists of a silicon vertex detector system for the precise measurement of secondary vertices, a central outer tracker, a time of flight detector within a 1.4T magnetic field generated by a super conducting solenoid. Outside that, there are electro-magnetic and hadron calorimeters, and a muon detector system at the outermost side for identification of muons.

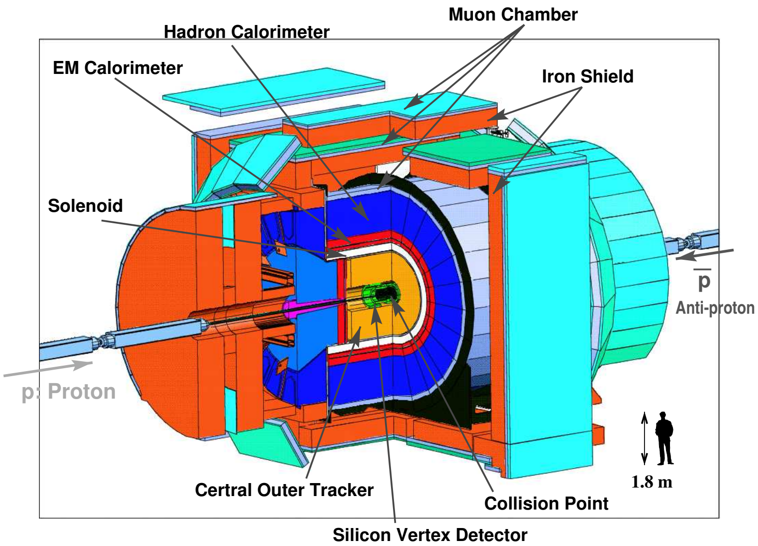

Figure 1. Schematic of the CDF IIa detector.

After the successful Run I from 1992 to 1996, in which CDF collected about 109 pb^{-1} in the integrated luminosity, we are now in a new data taking period, Run II started in March 2001 with the new detector system described above.

So far (middle of December, 2002), we have collected data corresponding to an integrated luminosity of about 80 pb^{-1} as good physics runs, of which 60 pb^{-1} is obtained while the silicon detector was functioning well. Run IIa will last until end of 2004, and the luminosity goal for Run IIa is $2\,\mathrm{fb}^{-1}$. There will be 6-month shutdown to upgrade to Run IIb in early 2005. The goal of the total luminosity in Run IIa and Run IIb is $15\,\mathrm{fb}^{-1}$.

In the Standard Model (SM), the top quark had been expected to be a partner of the b-quark in a SU(2) doublet of weak isospin in the third generation, and was discovered by CDF and DØ in 1995[1, 2]. Special features of the top quark are its large mass and width. The mass is measured to be in the range of 175 GeV/c^2 and the width is calculated to be about 1.42 GeV[3]. Therefore the top quark is expected to decay much faster than the spin-flip time due to hadronization[4]. This property provides us an opportunity to probe the spin polarization of the top quark. In addition, the top quark has almost "natural" Yukawa coupling $\sqrt{2}\, m_t/v$, which gives us a hint that the top quark might play a special role in the electro-weak symmetry breaking.

At Tevatron, the top quark is produced mainly in the following two mechanisms. One is the $t\bar{t}$ pair production through the strong interaction. Fig.2 shows the diagrams of these processes. The other is the single top quark production via the electroweak interaction, which is shown in Fig. 3. In the former production mechanism, a dominant contribution to the $t\bar{t}$ production is the $q\bar{q}$ annihilation process, and an about 10% contribution comes from the gluon fusion processes. On the other hand, dominant contributions to the single top production are the s-channel W^* exchange process and the W-gluon fusion process[5].

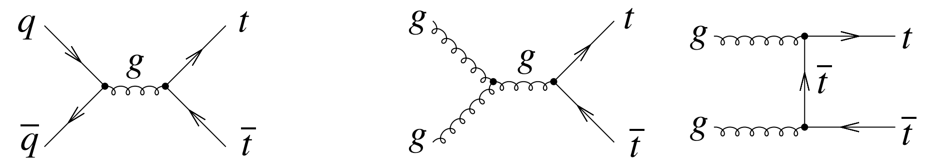

Figure 2. The lowest-order Feynman diagrams for the $t\bar{t}$ pair production through the strong interaction. The left one is the most dominant contribution to the $t\bar{t}$ production, namely, the $q\bar{q}$ annihilation process. The other two are the gluon fusion processes.

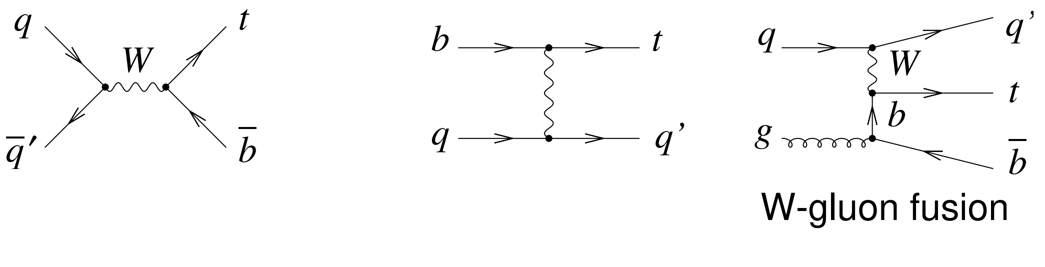

Figure 3. The lowest-order Feynman diagrams of the single top production. The left two show virtual time-like and space-like W-boson exchange processes, respectively. The other one is the W-gluon fusion process.

In SM, the top quark goes $W + b$ at a rate of almost 100%. So we can classify decay channels of a $t\bar{t}$ pair into the following three categories according to W decay channels as shown in Table 1.

$t \to W^+ b$			
$\hookrightarrow$	$\ell^+\nu$	$q\bar{q}'$ $\ell^+\nu$	$q\bar{q}'$
$\bar{t} \to W^- \bar{b}$			
$\hookrightarrow$	$\ell^-\bar{\nu}$	$\ell^-\bar{\nu}$ $q\bar{q}'$	$q\bar{q}'$
	dilepton	lepton + jets	all hadronic

Table 1. Three categories of decay channels from a $t\bar{t}$ pair.

The first category is labeled as dilepton channel, where two leptons, two jets, and missing transverse energy($\not{E}_T$) can be observed. The second is lepton+jets channel, where one lepton, four jets, of which at least two jets are originated from b- and $\bar{b}$-quarks, and $\not{E}_T$ can be observed. The last is all hadronic channel. The branching fractions to each channels are shown in the Table 2, which can be calculated with the branching fractions of W decay modes[6]. Leptons in the table denote only electrons, muons, and their anti-particles. Because of a quite different identification way of the τ particles, any decay channels including τ's are classified into another category in the table. The largest fraction is all-hadronic channel, but it generally has a considerable amount of QCD backgrounds. The second largest fraction is the lepton+jets channels. The last one is the dilepton channels which provide a particularly clean sample of $t\bar{t}$ events, though only 5% contribution comes from these channels.

dilepton			lepton+jets		all hadronic	τ+X
e+e	e+μ	μ+μ	e+jets	μ+jets	44%	21%
1%	2%	1%	15%	15%		

Table 2. Branching fractions to each decay channels of $t\bar{t}$.

2 Top Physics Results in CDF Run I

2.1 $t\bar{t}$ production cross section

One of theoretical questions deserving of attention is the quantitative reliability of cross sections based on the main production mechanism in perturbative QCD, namely $t\bar{t}$ production. CDF measured the $t\bar{t}$ production cross section in four independent samples in Run I, respectively, and obtained $\sigma_{t\bar{t}} = 6.5^{+1.6}_{-1.4}$ pb as a combined result of the four measurements[7]. The resultant cross sections are shown in Fig. 4, in which CDF assumed $M_t = 175\,\mathrm{GeV}/c^2$. Fig. 5 shows the mass of the top quark and the $t\bar{t}$ production cross section acquired by both CDF and DØ in Run I together with several theoretical predictions, in which the next-to-leading order (NLO) and the soft gluon re-summation are considered in calculations[8, 9, 10]. The experimental results are in good agreement with predictions.

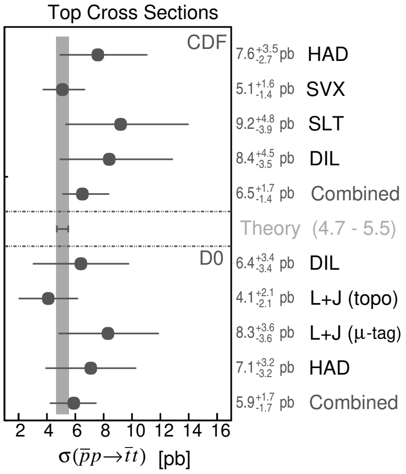

Figure 4. $t\bar{t}$ production cross section measurements with error bars in several independent channels in CDF Run I. The results in the all hadronic, lepton+jets(SVX and Soft Lepton tagged), and dilepton channels and the combined result of these four are shown, also together with those from DØ and the range of theoretical predictions, respectively.

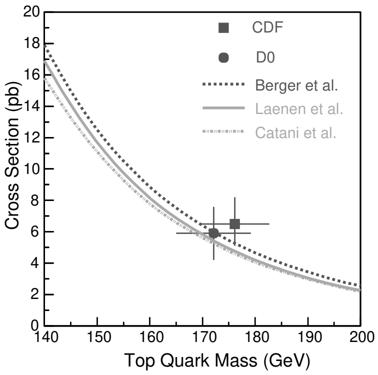

Figure 5. Square dots in the figure show the range of mass and cross section measured in Run I at CDF and DØ, respectively. The dotted, solid and dashed curves in the figure show several theoretical predictions.

2.2 Top quark mass

CDF performed the top quark mass measurements in the lepton+jets, dilepton, and all hadronic channels in Run I. In the lepton+jets channel, for example, CDF assumes that each event in the samples contains a pair of massive particles with the same mass (m_t), which subsequently decay as predicted in SM, and a neutrino of which transverse momenta are equal to $\not{E}_T$ of the event, and then defined a χ^2 using all the kinematical variables which are experimentally observable and assumed parameters, i.e. longitudinal momentum of the neutrino (p_z^ν), and m_t. By minimizing the χ^2, a m_t can be extracted as a reconstructed top quark mass in an event. Fig. 6 shows the distribution of the reconstructed top quark mass, with predicted distributions of both the $t\bar{t}$ signal and any backgrounds by Monte Carlo simulations. Performing a maximum likelihood fit of the data distribution to the predicted distribution with an assumed m_t, CDF obtained $175.9 \pm 4.8(\mathrm{stat}) \pm 4.9(\mathrm{syst})\ \mathrm{GeV}/c^2$ as the measurement of the top quark mass in lepton+jets channel. The negative log-likelihood is given as a function of assumed m_t at the inset in Fig. 6 as well.

In the lepton+jets channel, there is a sufficient number of kinematical constraints to solve unknown parameters. In the dilepton channel, however, two neutrinos are missing, and the system of kinematical observables in an event is underconstrained. The CDF adopted a neutrino-momentum weighting technique[11], where a distribution of the pseudo-rapidities of the two neutrinos is supposed to be known, and assuming the top quark mass and the two neutrino pseudo-rapidities in an event. On this assumption the event is completely constrained and can be solved for the top and anti-top momenta. Different solutions are weighted by how well they reproduce the measured $\not{E}_T$, and weighted according to the assumed neutrino pseudo-rapidity distributions as well.

In addition, CDF performed kinematical fits using a sample of the all hadronic events selected using SVX tagging[12]. All results are summarized in Fig. 7. The results for the three channels have been combined to yield a single CDF measurement. The three statistical uncertainties were taken as uncorrelated, while the systematic uncertainties were assumed to be either 0% correlated or 100% correlated between any pair of channels. The primary systematic uncertainty, that due to the jet energy scale, was taken as 100% correlated between all pairs, as was the signal model (mostly due to initial and final state radiation) and MC generator. The resultant top quark mass from the CDF combined measurement is 176.1 ± 6.6 GeV/c^2[11]. The Tevatron (CDF+D∅) Run I average in the figure was obtained by combining five CDF and D∅ results in a similar manner to the way the CDF and D∅ averages were obtained.

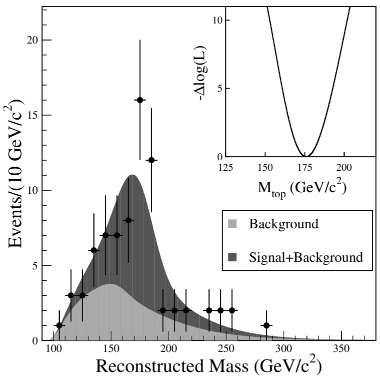

Figure 6. Reconstructed top quark mass distribution obtained based on 76 $t\bar{t}$ lepton+jets channel candidates in CDF in Run I. The Monte Carlo $t\bar{t}$ (assuming top mass 175.9 GeV/c^2) and background distributions are superimposed, with the normalization given by the best likelihood fit. The inset shows the shape of the negative log-likelihood as a function of the top quark mass.

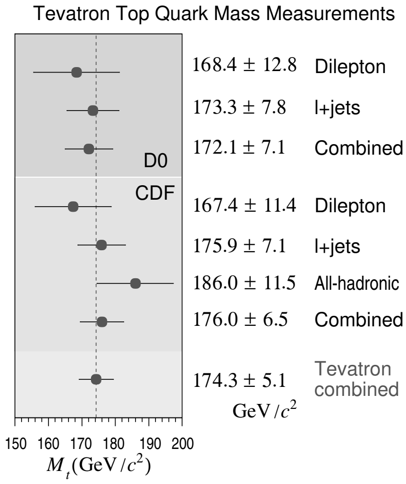

Figure 7. CDF and D∅ results of the top quark mass measurements in Run I. The figure shows results in several independent channels of $t\bar{t}$ and combined results of them. Also the Tevatron average for Run I is plotted in the figure, obtained by combining five CDF and D∅ results.

The top quark mass m_t is a crucial input parameter for the tests of the electroweak theory, since radiative corrections to many precision electroweak observables are sensitive to m_t. Comparing the experimental constraints on the W mass (M_W) and m_t with the SM prediction[13] for $M_W(m_t, m_{\text{Higgs}})$ tests the consistency of the SM. Fig. 8 shows the constraint on the Higgs mass obtained from the measurements on M_W and m_t in CDF Run I and other experiments.

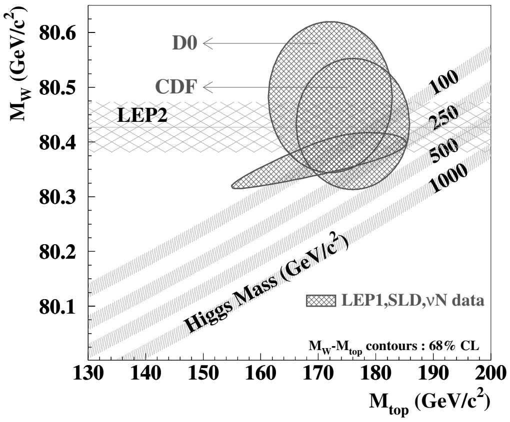

Figure 8. 68% C.L. region from measurements on the W mass and the top mass at CDF Run I, and other experiments. The curves in the figure are given by a calculation of the dependence of the W mass and the top mass in SM assuming several Higgs masses. The bands of the curves represents uncertainties in the theoretical calculation.

2.3 *W* helicity in top decay

The Standard Model predicts the top quark decays only to longitudinally polarized (zero-helicity) or left-handed (negative-helicity) W bosons, and the fraction to longitudinal W bosons ($\mathcal{F}_0$) are considerably large due to the large mass of the top quark. The right-handed (positive-helicity) W bosons are strictly forbidden if we neglect the b quark mass. At the leading order calculation, the fraction to longitudinal W is given by

$$\mathcal{F}_0 \equiv \frac{\Gamma(h_W=0)}{\Gamma(h_W=0)+\Gamma(h_W=-1)} = \frac{m_t^2/2m_W^2}{1+m_t^2/2m_W^2} \approx 0.70$$

By measuring this fraction, therefore, we can make experimental test of the $V-A$ coupling and/or search for anomalous couplings in the t-W-b vertex.

Experimentally, one can use the p_T distributions of the leptons in the top quark decays to distinguish the three helicity states of the W bosons, since angular distributions of the leptons from the W bosons are different according to the W helicities as follows:

$$\begin{aligned}
|\mathfrak{M}(W_{\text{left}})|^2 &\propto \frac{1}{4}(1-\cos\theta_l^*)^2 \\
|\mathfrak{M}(W_{\text{long}})|^2 &\propto \frac{1}{2}(\sin\theta_l^*)^2 \\
|\mathfrak{M}(W_{\text{right}})|^2 &\propto \frac{1}{4}(1+\cos\theta_l^*)^2,
\end{aligned}$$

where θ_l^* denotes an angle of a lepton flight direction in a W rest frame with respect to the W flight direction in a top rest frame as shown in Fig. 9. The plots in Fig. 10 show the reconstructed p_T distributions of leptons in the top quark decays, corresponding to W helicity states using a simulation.

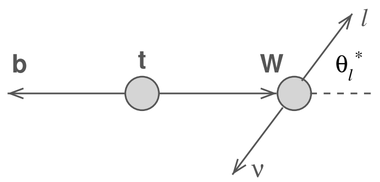

Figure 9. Schematic of the semi-leptonic decay of a top quark. θ_l^* is defined as an angle between a W flight direction in a top rest frame and a lepton flight direction in the W rest frame.

CDF has measured the lepton p_T spectra for the dilepton and lepton+jets channels[14]. By assuming no positive-helicity W's are present, CDF obtained the fraction $\mathcal{F}_0 = 0.91 \pm 0.37(\text{stat}) \pm 0.12(\text{syst})$ as shown in Fig. 11, and by setting $\mathcal{F}_0$ to the SM value of 0.70 obtained $\mathcal{F}_+ = 0.11 \pm 0.15(\text{stat}) \pm 0.06(\text{syst})$ as the fraction to right-handed W's.

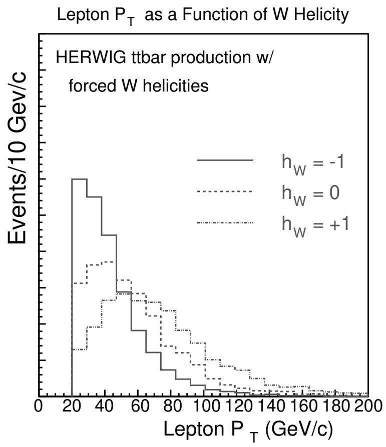

Figure 10. Simulated p_T distributions of the leptons in the semi-leptonic decay of the top quark, assuming the negative, zero, and positive helicity of the W bosons, respectively. A modified version of the HERWIG Monte Carlo, is used to create these plots. The top mass used in the simulation is $175\,\text{GeV}/c^2$.

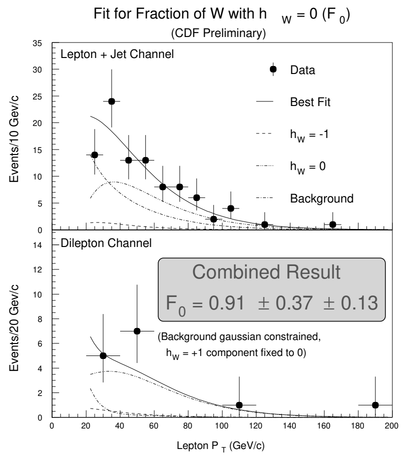

Figure 11. The plots shows reconstructed p_T distribution in the lepton+jets (upper) and dilepton (lower) channels. The dots indicate CDF Run I data, and curves the simulated p_T distributions. The fits are performed for the lepton p_T distributions on the hypothesis that the W bosons have helicities of either -1 or 0 in the top rest frame. The fits extract the fraction of zero-helicity W's.

2.4 Search for single top production

The single top quark production always involves the t-W-b vertex through the electroweak interaction. This provides us the only known way to directly measure the CKM matrix element $|V_{\text{tb}}|$ at hadron colliders. As mentioned above, the dominant contributions come from s-channel W^* and W-gluon fusion. The experimental event signatures these two processes are as follows:

W-gluon fusion a W decay, hard b-jet, soft b-jet and light quark jet which is usually at high pseudo-rapidity (η). The soft b-jet is from a gluon splitting, which has low E_T and is undetected in most cases.

s-channel W^* a W decay and two hard b-jets.

CDF performed a search for the single top quark production in 106 pb^{-1} of Run I data[15], selecting events with a lepton, missing energy, and 1, 2, or 3 jets, of which at least one jet is b-tagged. After a cut on the reconstructed mass of $140 < M_{\ell\nu b} < 210$ GeV/c^2 is applied, CDF observed 65 candidate events, while the SM expectation is 67 ± 12 events (3.0 W-gluon fusion, 1.3 s-channel W^*, 8.4 $t\bar{t}$ and 54 non-top events mainly originate from QCD backgrounds). To distinguish each components of the data sample, CDF looked at H_T which is defined as the total sum of transverse energies of all the decay products in an event, i.e.

$$H_t \equiv |\not{E}_T| + |E_T(\ell)| + \sum |E_T(\text{all jets})| .$$

The H_T inclines to go higher if there are any particles with a large mass in an event. Performing an unbinned maximum likelihood fit to the H_T distribution yielded an upper limit on the single top production cross section of 14 pb, while the Standard Model predicts 2.4 pb. Fig. 12 shows the reconstructed H_T distribution after all the selections in Run I data, together with the SM predictions of QCD backgrounds, single top signals, and $t\bar{t}$ backgrounds, adopting the best fit results as each normalizations.

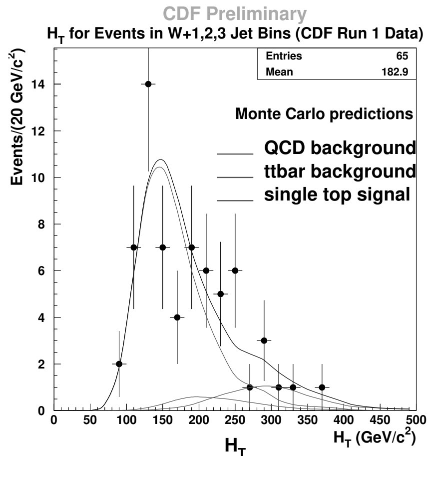

Figure 12. Reconstructed H_T distribution. Dots indicates the data. Three curves correspond to the SM predictions of QCD backgrounds, single top signals, and $t\bar{t}$ backgrounds, respectively, using the best fit normalizations.

2.5 Other results on top physics in CDF Run I

Though there are other various interesting analyses on the top physics in Run I, we mention only briefly the following topics:

- Measurement of Branching ratio $R = \dfrac{\mathrm{Br}(t \to Wb)}{\mathrm{Br}(t \to Wq)}$.

  In the SM, R is supposed to be close to 1. CDF has measured $R = 0.94^{+0.31}_{-0.24}$[16]. Assuming three generations of quarks, this ratio constrains $|V_{\mathrm{tb}}| = 0.97^{+0.16}_{-0.12}$ or $|V_{\mathrm{tb}}| > 0.76$ at 95% C.L. On the assumption of three generations, however, the much more rigid constraint, $0.9991 < |V_{\mathrm{tb}}| < 0.9994$ has been given by data on the light quarks combined with CKM unitarity[6].

- Search for FCNC top quark decays.

  Flavour-changing neutral currents in the top decay are strongly suppressed in SM due to so-called GIM mechanism. $t \to u/c + \gamma$ or $t \to u/c + Z^0$ are, for example, predicted to have branching fractions less than 10^{-10}. So if these decay modes are observed at a higher branching fraction, it is a symptom of a new physics at once. CDF searched these processes in $p\bar{p} \to t\bar{t} + X$ candidate events[17] and obtained the following results:

  - $\mathrm{Br}(t \to u/c + \gamma) < 3.2\%$ (95%CL)
  - $\mathrm{Br}(t \to u/c + Z^0) < 33\%$ (95%CL)

3 Status of Top Physics Analysis in CDF Run II

As of mid-December 2002, the accelerator has delivered about 150 pb^{-1} of integrated luminosity, with about 100 pb^{-1} being recorded. Of that, CDF currently has about 80 pb^{-1} of good data for analysis. The baseline goal of the accelerator through to October 2003 is to deliver 10 pb^{-1} per week, translating to an expected data sample of about 200 pb^{-1} of good data by October 2003, about twice the integrated luminosity of Run I.

We will present the first preliminary top physics results from Run II in March 2003. These will include $t\bar{t}$ cross section in both the dilepton and lepton+jets channels, and top mass measurements in lepton+jets channel as well. Fig. 13 shows a candidate event in the $t\bar{t}$ dilepton channel.

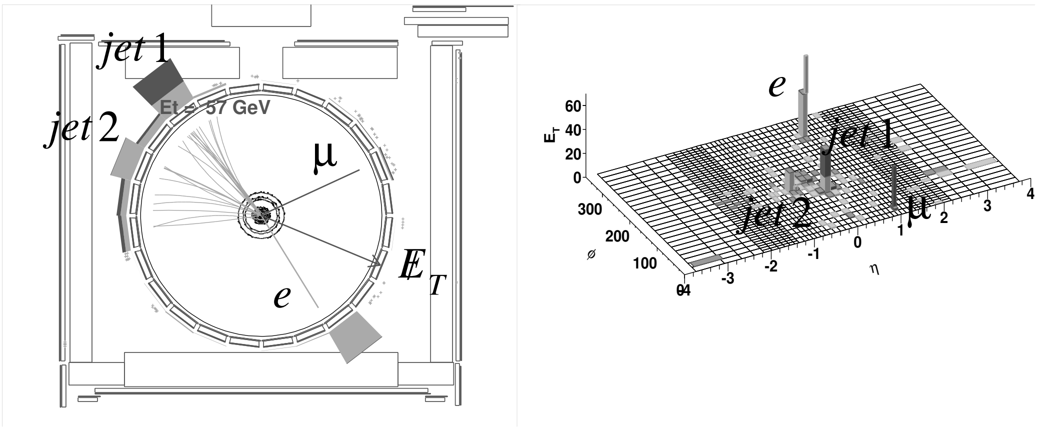

Figure 13. A $t\bar{t}$ dilepton candidate in Run II. Left: A cross-sectional drawing on the plane perpendicular to the beam axis. Colored cells indicate energy deposit on the calorimeters. You can see e, μ, two jets, and large $\not\!\!E_T$. Right: Energy deposits in the calorimeters on the two-dimensional plane of pseudo-rapidity (η) v.s. azimuth (ϕ). Run 156484, Event 3099305, $E_T(e) = 34\,\mathrm{GeV}$, $E_T(\mu) = 36\,\mathrm{GeV}$, $E_T(\mathrm{jets}) = 57, 28\,\mathrm{GeV}$, $\not\!\!E_T = 55\,\mathrm{GeV}$, $M_{e\mu} = 47\,\mathrm{GeV}$, $H_T = 227\,\mathrm{GeV}$.

4 Top Physics Prospects in CDF Run II

Here we discuss about the prospects on the top physics possible in the CDF Run II period. Table 3 summarizes the parameters related to the top physics and yields of the top quark events expected in Run I, Run IIa and Run IIb, respectively. Table 4 summarizes Run I results and precisions of measurements expected in Run IIa and Run IIb for some of the studies of top quark physics. Uncertainty in cross section will reduce to 10% for Run IIa and 5% for Run IIb. We'll observe 100 or 200 single top events in Run IIa. We also improve the accuracy in the measurement of W helicity in top decay and the sensitivity of search for FCNC top decay.

	Run I	Run IIa	Run IIb
CM Energy (TeV)	1.8	1.96	1.96
Integrated Luminosity (fb^{-1})	0.11	2.0	15.0
Production			
$\sigma_{t\bar{t}}$ (pb)	5.0	7.0	7.0
$\sigma_{\mathrm{single}\,t}$ (pb)	2.5	3.4	3.4
Number of $t\bar{t}$ produced	500	14000	105000
Number of single t produced	250	7000	52500
Yields			
dilepton channel	4	150	1100
$N(t\bar{t} \to \ell + \geqslant 3j)(\geqslant 1\ b\text{-tag})$	25	1400	10000
$N(t\bar{t} \to \ell + \geqslant 4j)(2\ b\text{-tag})$	5	600	4500
$N(\text{single t})\ (W + 2j\ \text{w/ } 1\ b\text{-tag})$	3	140	1000

Table 3. Summary of parameters related to the top physics and yields of the top quark events expected in Run I, Run IIa and Run IIb, respectively.

		Run I result	Run I	Run IIa	Run IIb
Mass	m_t	$176.1 \pm 6.6\,\mathrm{GeV}$	6.6 GeV	2-3 GeV	1-2 GeV
cross section	$\sigma_{t\bar{t}}$	$6.5^{+1.7}_{-1.4}\,\mathrm{pb}$	25%	10%	5%
Whelicity	$\mathcal{F}_0$	$0.91 \pm 0.37 \pm 0.13$	0.4	0.09	0.04
	$\mathcal{F}_+$	$0.11 \pm 0.15 \pm 0.06$	0.15	0.03	0.01
$R \equiv \frac{B(t \to Wb)}{B(t \to \mathrm{Wq})}$		$0.94^{+0.31}_{-0.24}$	30%	4.5%	0.8%
$\sigma_{\mathrm{single}-t}$		$< 13.5\,\mathrm{pb}$	–	20%	8%
$\lvert V_{\mathrm{tb}} \rvert$ from	single-t	–	–	12%	5%
FCNC decay	$B(t \to \gamma q)$	< 0.03 (95% C.L.)	< 0.03	?	?
	$B(t \to \mathrm{Z}q)$	< 0.32 (95% C.L.)	< 0.3	< 0.02	?

Table 4. Summary of Run I results and expected uncertainties of measurements in Run IIa and Run IIb on physics topics related to the top quark.

The dominating systematic uncertainty in the top quark mass measurement in Run I comes from the jet energy scale and the modeling of initial-state and final-state radiations. With the increased integrated luminosity, the systematic effects will dominate uncertainties in the measurements of $\sigma_{t\bar{t}}$ and m_t. The error on m_t is estimated to reach 2-3 GeV/c^2 in Run IIa, which gives more powerful constraint for Higgs mass. Uncertainty of higgs mass will reach to about 40%. Fig. 14 shows an estimation of 68% C.L. allowed region on M_W and m_t plane for $2\mathrm{fb}^{-1}$.

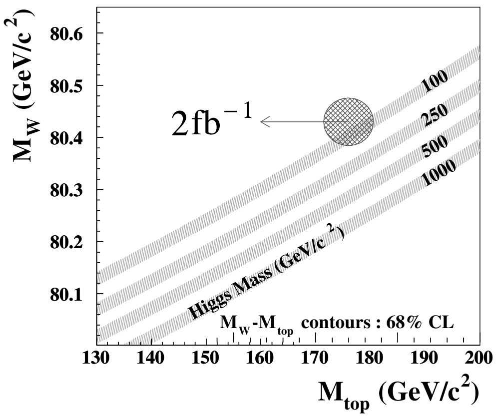

Figure 14. 68% C.L. region expected at measurements on W mass and top mass in CDF Run IIa, i.e. for integrated luminosity of $2\mathrm{fb}^{-1}$.

One of the interesting topics expected to be feasible in Run IIa is on $t\bar{t}$ spin correlations, which is expected to be sensitive to some anomalous couplings in the $t\bar{t}$ pair production[18, 19]. Top quark decays before losing the spin information at production. About 90% of $t\bar{t}$ pairs produced at Tevatron come from $q\bar{q}$ annihilation as mentioned. It is possible to gain only like-spin combinations in the $t\bar{t}$ pair, namely 100% correlations, if we take an optimal spin quantization basis, so-called "Off-diagonal basis"[20]. Fig. 15 shows a spin configuration in a $t\bar{t}$ pair production event via $q\bar{q}$ annihilation.

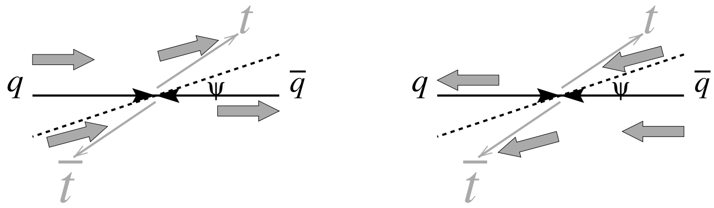

Figure 15. Spin configurations in the $t\bar{t}$ pair production from the $q\bar{q}$ annihilation. If we choose the off-diagonal basis (the broken line in the figure) as a spin quantization basis of the top and anti-top quarks, the spins of the $t\bar{t}$ pair are 100% correlated.

The spin of the top quark can be measured by a lepton flight direction in the top quark rest frame. We can look at spin correlations as correlations between angular distributions of the flight directions of leptons from the top and anti-top quarks. Fig. 16 shows the angular correlations using a Monte Carlo generator. Recently a calculation on the spin correlations, in which NLO is taken into account was presented[21]. Run IIa will provide us a good opportunity for observing the $t\bar{t}$ spin correlations.

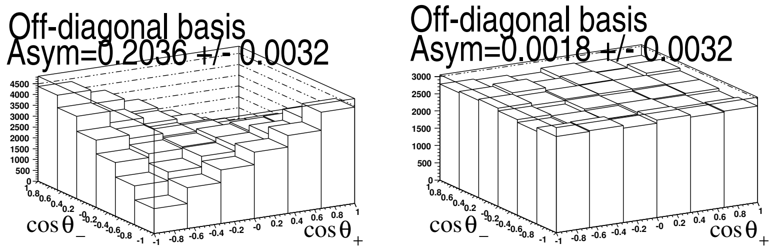

Figure 16. Angular correlation distributions of samples generated by an event generator (HERWIG 6.5) with (left) and without (right) the spin correlations.

5 Conclusion

CDF had the successful top quark physics programs in Run I. All measurements in Run I are consistent with the Standard Model, but they are limited in statistics. We are now entering an exciting period of Run II, where precise measurements on the top physics are about to begin. We have now the amount of data, comparable to Run I, and some of the first results on the top physics in Run II will come very soon (actually came in this March). Run II is promised to be prolific of the top quarks, and will give us much information about top quark before LHC and the linear collider era.

Acknowledgments

The author would like to thank the organizer of this institution. The author acknowledges receipt of Research Fellowships of the Japan Society for the Promotion of Science for Young Scientists.

Bibliography

[1] S. Abachi et al., Phys. Rev. Lett. **74**, 2632(1995).

[2] F. Abe et al., Phys. Rev. Lett. **74**, 2626(1995).

[3] M. Beneke et al., CERN-TH/2000-100.

[4] T. Stelzer and S. Willenbrock, hep-ph/9512292.

[5] B. W. Harris et al., hep-ph/0207055.

[6] K. Hagiwara et al., Phys. Rev. **D66**, 1–974(2002).

[7] F. Abe et al., Phys. Rev. Lett. **80**, 2773(1998).

[8] R. Bonciani et al., Nucl. Phys. **B529**, 424(1998).

[9] E. Laenen, J. Smith, and W.L. an Neerven, Phys. Lett. **B321**, 254–258(1994).

[10] E.L. Berger and H. Contopanagos, Phys. Rev. **D54**, 253–264(1998).

[11] F. Abe et al., Phys. Rev. Lett. **82**, 271(1999).

[12] F. Abe et al., Phys. Rev. Lett. **79**, 1992(1997).

[13] G. D'Agostini and G. Degrassi., Eur. Phys. J. **C10**, 663–675(1999).

[14] T. Affolder et al., Phys. Rev. Lett. **84**, 216(2000).

[15] D. Acosta et al., Phys. Rev. **D65**, 091102(2002).

[16] T. Affolder et al., Phys. Rev. Lett. **86**, 3233(2001).

[17] F. Abe et al., Phys. Rev. Lett. **80**, 2525(1998).

[18] B. Holdom and T. Torma, hep-ph/9906208.

[19] K. Ohkuma, hep-ph/0105117.

[20] G. Mahlon and S. Parke, Phys. Lett. **B411**, 173–179(1997).

[21] W. Bernreuther, A. Brandenburg, Z.G. Si, and P. Uwer., hep-ph/0209202.